Crack onset at a v-notch. Influence of the notch tip radius

Dominique Leguillon, Zohar Yosibash

Crack onset at a v-notch. Influence of the notch tip radius

DOMINIQUE LEGUILLON[1] and ZOHAR YOSIBASH[2],

[1]Laboratoire de Modélisation en Mécanique - CNRS UMR 7607, Université Pierre et Marie Curie, Paris, France
[2]Division of Applied Mathematics, Brown University, Providence, U.S.A.

Abstract. A criterion to predict crack onset at a sharp notch in homogeneous brittle materials has been presented in a previous paper of one of the authors. It is reviewed and improved herein. It fulfils both the energy and the strength criteria and takes an Irwin-like form involving the generalized intensity factor of the singularity governing the elastic behaviour in the vicinity of a notch tip. The prediction agrees fairly well with the experiments although it slightly underestimates the experimental measures. A cause of this discrepancy can be that a small notch tip radius blunts the sharp corner. It is analysed in this paper by means of matched asymptotics involving 2 small parameters: a micro-crack increment length and the notch tip radius. A correction is brought to the initial prediction and a better agreement is obtained with experiments on PMMA notched specimens. Experiments performed on a stiffer material (Alumina/Zirconia) show that it is less sensitive to small notch tip radii. A remaining small discrepancy between experiments and predictions can be due to some non linear behaviour of the materials near the notch tip. In addition, without new developments, the method allows to determine the stress intensity factor at the tip of a short crack emanating from a sharp or a rounded v-notch.

Key words: Elasticity, brittle fracture, v-notch, PMMA, Alumina

1. Introduction

One of the authors performed 3-point bending experiments on PMMA and Alumina-Zirconia (AZ) notched specimens (Yosibash et al., 2003). These tests allowed him to check the prediction capacity of different failure criteria. One of these was proposed by the other author in a previous paper (Leguillon, 2002) to predict crack onset at sharp notches in homogeneous brittle materials. In plane elasticity, it is of the Irwin form

$$k \geq k_c \ , \tag{1}$$

where k is the generalized intensity factor (also called GSIF) of the singular term governing the elastic behaviour near the notch tip, i.e. the factor $k = k_1$ of the most singular term in an expansion of the elastic solution in power terms

$$\underline{U}(x_1, x_2) = \sum_i k_i r^{\lambda_i} \underline{u}^i(\varphi) \ , \ 0 < \lambda_1 \leq \lambda_2 \leq \dots \ , \tag{2}$$

where r and φ are polar coordinates with origin at the notch tip, see Section 2.1 for more details.
The critical value k_c can be expressed in terms of the strength σ_c, the toughness G_c of the material, the singular exponent λ ($= \lambda_1$ in (2)) and a scaling coefficient $\bar{K}$

*On Sabbatical leave from the Department of Mechanical Engineering, Ben-Gurion University of the Negev, Beer-Sheva 84105, Israel

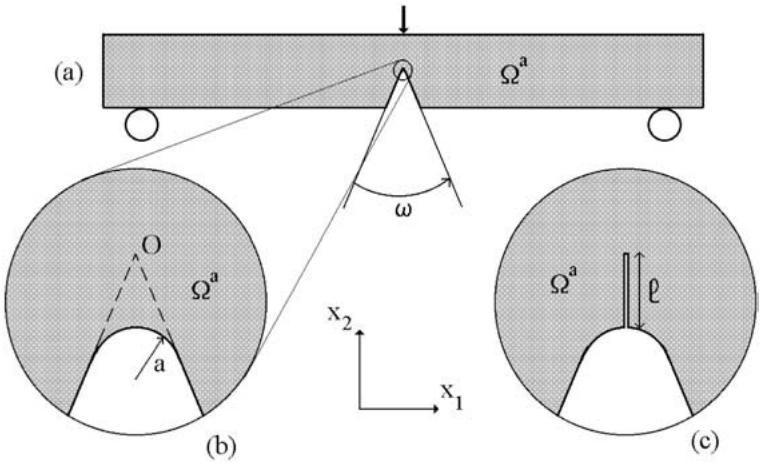

Figure 1. (a) The 3-point bending test on a notched specimen, (b) the notch tip radius a, (c) the short additional crack with length ℓ.

$$k_c = \left(\frac{G_c}{\bar{K}}\right)^{1-\lambda} \sigma_c^{2\lambda-1} \ . \tag{3}$$

It enjoys the desirable property to coincide with the Griffith criterion for a crack ($\lambda = 0.5$) and with the strength criterion for a straight edge ($\lambda = 1$). It has been shown that the proposed failure criterion (the predicted k at failure) is in good agreement with the experimental observations (k_c measured at the instant of failure (Yosibash et al., 2003)), but slightly underestimates it. This is for one part a consequence of the assumption that the V-notch tip is sharp whereas, in reality, a small radius exists at the tip. The derivation of the failure criterion for a sharp v-notch is briefly reviewed in Section 3 where an improved calculation of the scaling term $\bar{K}$ involved in relation (3) is proposed. Results agree fairly well with experiments (Dunn et al., 1997; Yosibash et al., 2003) respectively on PMMA and AZ specimens, as will be discussed below (see Sections 4.2 and 4.3). Extensions to non-homogeneous situations: failure of a butt or scarf joint (Leguillon, 2002) with a comparison with experiments (Reedy and Guess, 1993, 1997, 1999; Qian and Akisanya, 1998), failure of a bimaterial wedge (Leguillon and Siruguet, 2002) again with a comparison with experiments (Mohammed and Liechti, 2000), prove the generality of the criterion although the presence of different materials makes the analysis more complex.

Nevertheless, Figure 11 in Section 4.2 shows that the predicted values slightly underestimate the experimental ones in PMMA specimens particularly. For the notch openings $\omega = 60°$, $90°$ and $120°$, a notch tip radius reported to be around 25.4 μm by the authors of the experiments can be the cause of this small discrepancy. The influence of such a notch tip blunting is analyzed in the present paper by means of matched asymptotics (Section 2). The solution is split in two connected parts: a far field ignoring at the leading orders any small geometrical perturbation (blunting, new micro-crack), i.e. with an apparent sharp notch, and a near field defined in the vicinity of these perturbations. The two fields must match in an intermediate area. The knowledge of the near field allows, first to calculate the potential energy change due to the nucleation of a micro-crack of length ℓ, and second to know precisely the influence of the rounding on the tension acting in the material along the anticipated path of the new crack. They are the necessary elements to extend the criterion (1) to this special case of blunting.

This kind of analysis, based on the change in potential energy, is sometimes baptised 'Finite Fracture Mechanics' (Hashin, 1996). It is almost rough, no description of a continuous process between 0 and ℓ is necessary. At this step ℓ is an unknown parameter, it must be small (asymptotic assumption) but cannot be infinitely small, the energy balance gives a lower bound to this length that vanishes only for a sharp crack tip. The generally non zero lower bound shows that the first stage of propagation is a sudden process. The crack length is assumed to jump from 0 to $\ell = \ell_0$ determined by a stress argument: the tension must be above the strength σ_c all along the anticipated crack path, i.e. from 0 to ℓ_0.

The aim is not to perform a thorough phenomenological analysis of the crack onset at a v-notch that needs to account for actual fracture mechanisms including plasticity (and crazing in PMMA). On the contrary, the study do not enter into the details and proposes a simple and robust criterion to predict crack initiation at v-notches in brittle materials. It is based on elasticity, requires few material parameters and seems to give quite satisfactory predictions. It can be included for instance in a FE code to optimize the design of structures. Indeed, plasticity and crazing take place also at the tip of long cracks in PMMA, however the Griffith criterion, based on elasticity and a very simple energy argument, gives good approximations in the prediction of growth of such cracks. One reason is probably that in small scale yielding materials the toughness G_c, measured in a DCB test for instance, contains a large part of the plastically dissipated energy. As a well-known fact, G_c does not reduce to the reversible surface energy. It is observed in this paper that the correction accounting for a small notch tip radius still underestimates the measures. The remaining small discrepancy is certainly due to these neglected or averaged non linear effects.

Finally it is found that the predicted values using the sharp notch criterion must be increased by 13.5%, 11% and 4.7%, respectively, for $\omega = 60°$, $90°$ and $120°$ in PMMA. Similar conclusions are drawn from a comparison with experiments on AZ specimen (Yosibash et al., 2003) although, the material being stiffer, it seems to be less sensitive to small notch tip radii. Such an analysis provides also the threshold value of the v-notch tip radius (for each material) that does not influence the failure criteria.

In addition, without new developments, the method allows to determine the stress intensity factor at the tip of a short crack emanating from a sharp or a rounded v-notch (Section 2.5).

2. Matched asymptotics

The major difficulty in applying the usual procedure of matched asymptotic expansions lies in the presence of two competing small (with respect to the notch depth for instance) parameters: the notch tip radius a and the new micro-crack increment length ℓ. In the framework of crack nucleation these two parameters are not independent and moreover they play different roles in the asymptotics. To highlight this point the solutions to the two problems (i.e., prior to and following the onset of a short crack) write respectively

$$\underline{U}^a(x_1, x_2, 0) \text{ and } \underline{U}^a(x_1, x_2, \ell)\ . \tag{4}$$

Formally one of the small parameters is treated as a variable while the other is an index.

2.1. The far field

Mainly for practical reasons (as seen later in the remark at the begining of Section 2.5) we decide to expand (4) first with respect to the notch tip radius a. The far field is expressed as the

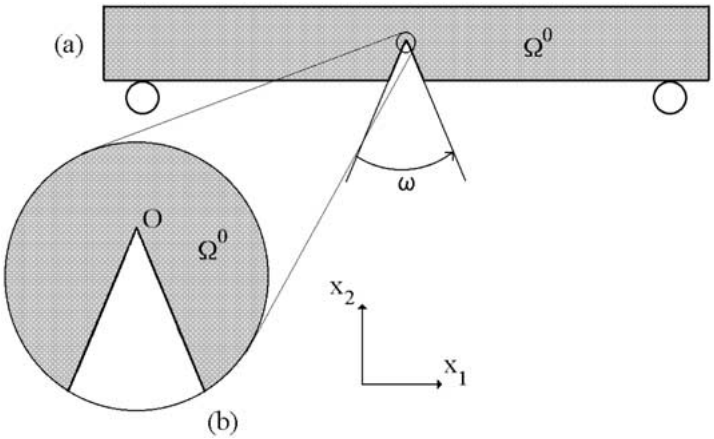

Figure 2. The unperturbed structure with a sharp notch tip.

solution $\underline{U}^0(x_1, x_2, \ell)$ to the unperturbed (i.e., without notch blunting: $a = 0$, see Figure 2) problem plus a small correction

$$\underline{U}^a(x_1, x_2, \ell) = \underline{U}^0(x_1, x_2, \ell) + f_1(a)\underline{U}^1(x_1, x_2, \ell) + \dots \ , \tag{5}$$

with $f_1(a) \to 0$ as $a \to 0$. The above expansion holds for $\ell = 0$ (no crack) and $\ell > 0$.

In the unperturbed domain Ω^0 (Figure 2), the notch tip is sharp, thus $\underline{U}^0(x_1, x_2, 0)$ undergoes the classical singularities

$$\underline{U}^0(x_1, x_2, 0) = \underline{U}^0(0, 0, 0) + k_1 r^{\lambda_1}\underline{u}^1(\varphi) + k_2 r^{\lambda_2}\underline{u}^2(\varphi) + \dots \ , \tag{6}$$

where r and φ are polar coordinates with origin at the notch tip. The characteristic exponents $1/2 \leq \lambda_1 < 1$ and $\lambda_2 \geq \lambda_1$ are associated respectively with a symmetric mode $\underline{u}^1(\varphi)$ and an antisymmetric one $\underline{u}^2(\varphi)$. The coefficients k_1 and k_2 are the associated generalized stress intensity factors (GSIF). Depending on the notch opening either $\lambda_2 < 1$ or $\lambda_2 \geq 1$. In the later case an intermediate term corresponding to $\lambda = 1$ (the rigid rotation) inserts in between in (6). However, in the present 3-point bending test problem, the antisymmetric terms do not play any role and in particular k_2 vanishes. Moreover, as a consequence of the symmetry properties of the specimen and of the loading, fracture occurs along the bisector ($\varphi = \pi - \omega/2 = \varphi_0$).
Remark: In the forthcoming equations we shall consider (6) with $k_2 = 0$ and simplified notations: $\lambda_1 = \lambda$, $\underline{u}^1(\varphi) = \underline{u}(\varphi)$ and $k_1 = k$

$$\underline{U}^0(x_1, x_2, 0) = \underline{U}^0(0, 0, 0) + k\ r^{\lambda}\underline{u}(\varphi) + \dots \tag{7}$$

In addition, the singular mode has been normalized in such a way that the tension acting along the bisector is $r^{\lambda-1}$

$$\sigma_n(r^{\lambda}\underline{u}(\varphi_0)) = \sigma((r^{\lambda}\underline{u}(\varphi_0)).\underline{n}.\underline{n} = r^{\lambda-1}s(\varphi_0).\underline{n}.\underline{n} = r^{\lambda-1} \ , \tag{8}$$

where $\underline{n}$ is the normal to the bisector. The quantities k, λ and the function $\underline{u}(\varphi)$ can be computed numerically (see for example (Leguillon and Sanchez-Palencia, 1987; Yosibash and Szabo, 1995)).

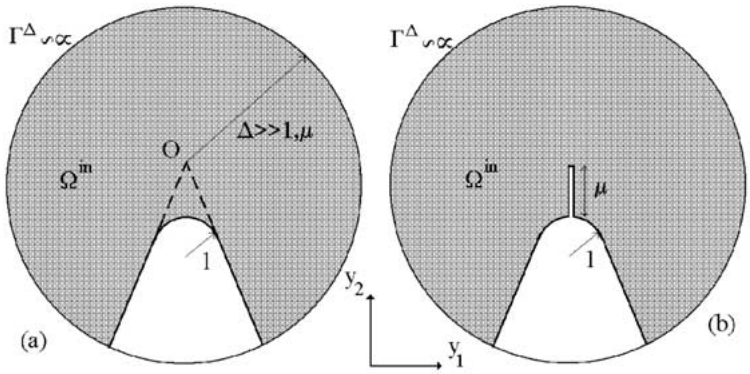

Figure 3. The unbounded domain Ω^{in}, (a) prior to any crack extension, (b) with a new small crack. The fictitious boundary Γ^Δ is extended to infinity.

2.2. THE NEAR FIELD

The previous expansion gives an accurate approximation of the solution far from the perturbation formed by the notch tip radius. Let us consider now the stretched dimensionless variables $y_i = x_i/a$ $(i = 1, 2)$. The notch tip radius is now 1 whatever its actual size. The change of coordinates assumes implicitly that ℓ is not infinitely large with respect to a. Then the (dimensionless) relative crack extension length defined by

$$\mu = \ell/a \tag{9}$$

remains finite.
Expanding $\underline{U}^a(x_1, x_2, 0)$ in the new variables allows to describe the near field

$$\begin{aligned} \underline{U}^a(x_1, x_2, 0) &= \underline{U}^a(ay_1, ay_2, 0) \\ &= F_0(a)\underline{V}^0(y_1, y_2, 0) + F_1(a)\underline{V}^1(y_1, y_2, 0) + \dots , \end{aligned} \tag{10}$$

with $F_1(a)/F_0(a) \to 0$ as $a \to 0$. The functions $\underline{V}^i(y_1, y_2, 0)$ are defined in an unbounded domain Ω^{in} (see Figure 3). Their behaviour at infinity is governed by the matching rules (Leguillon and Sanchez-Palencia, 1987): the near field (10) away from the perturbation must match the far field (7) approaching the corner. This conditions yield:

$$F_0(a) = 1 \; ; \; \underline{V}^0(y_1, y_2, 0) = \underline{U}^0(0, 0, 0) \tag{11}$$

and

$$F_1(a) = k\, a^\lambda \; ; \; \underline{V}^1(y_1, y_2, 0) = \rho^\lambda \underline{u}(\varphi) + \hat{\underline{V}}^1(y_1, y_2, 0) \; , \tag{12}$$

where $\rho = r/a$ and where $\hat{\underline{V}}^1(y_1, y_2, 0)$ is solution to a well-posed problem in the unbounded domain Ω^{in}. In particular, it decreases to 0 at infinity.

By analogy, considering a short crack at the rounded tip, the near field expands as

$$\begin{aligned} \underline{U}^a(x_1, x_2, \ell) &= \underline{U}^a(ay_1, ay_2, a\mu) \\ &= \underline{U}^0(0, 0, 0) + k\, a^\lambda[\rho^\lambda \underline{u}(\varphi) + \hat{\underline{V}}^1(y_1, y_2, \mu)] + \dots \end{aligned} \tag{13}$$

Remark: The functions $\underline{V}^1(y_1, y_2, \mu)$ (or $\underline{\hat{V}}^1(y_1, y_2, \mu)$) for μ equal to zero or not are independent of the applied loads. These applied loads intervene in (10) and (13) through the generalized intensity factor k thanks to $F_1(a) = k\, a^\lambda$ (see (12)).

2.3. The energy release rate

The initial state, prior to any crack nucleation, and the final one with a short additional crack, are described respectively by $\underline{U}^a(x_1, x_2, 0)$ and $\underline{U}^a(x_1, x_2, \ell)$. The change in potential energy δW between these two states can be expressed by a contour independent integral (Leguillon, 1989, 2002):

$$\delta W = \psi(\underline{U}^a(x_1, x_2, \ell), \underline{U}^a(x_1, x_2, 0)) \ , \tag{14}$$

where the definition of ψ relies on Betti's theorem

$$\psi(\underline{U}, \underline{V}) = \frac{1}{2} \int_\Gamma \left[\sigma(\underline{U}).\underline{N}.\underline{V} - \sigma(\underline{V}).\underline{N}.\underline{U}\right] dx \ . \tag{15}$$

Here Γ is any contour surrounding the crack, starting and finishing on the free edges of the notch, $\underline{N}$ its normal pointing inside the surrounded domain. The stress field associated with $\underline{U}$ is denoted $\sigma(\underline{U})$

$$\sigma(\underline{U}) = C : \nabla_x \underline{U}(x_1, x_2) \ , \tag{16}$$

where C is the elasticity matrix and ∇_x the (symmetric) gradient operator with respect to the space variables x_i.

The integral (14) can be computed either in the outer (unperturbed) domain spanned by x_1 and x_2 or in the inner one spanned by y_1 and y_2 (inner and outer refer to a vicinity of the perturbations). This later case is adopted, taking into account the expansion (13) used first with $\ell \neq 0$ and second with $\ell = 0$. Thanks to differerent properties of the integral (15), it is expressed finally at the leading order

$$\delta W = k^2 a^{2\lambda} [K(\mu) - K(0)] + \dots \ , \tag{17}$$

with

$$\begin{aligned} K(\mu) &= \psi(\underline{\hat{V}}^1(y_1, y_2, \mu), \rho^\lambda \underline{u}(\varphi)) \\ &= \psi(\underline{V}^1(y_1, y_2, \mu), \rho^\lambda \underline{u}(\varphi)) \ , \end{aligned} \tag{18}$$

since as in (12)

$$\underline{V}^1(y_1, y_2, \mu) = \rho^\lambda \underline{u}(\varphi) + \underline{\hat{V}}^1(y_1, y_2, \mu) \ . \tag{19}$$

Remark: The integral ψ computed in Ω^{in} is formally identical to (15)

$$\psi(\underline{U}, \underline{V}) = \frac{1}{2} \int_\Gamma \left[\tilde{\sigma}(\underline{U}).\underline{N}.\underline{V} - \tilde{\sigma}(\underline{V}).\underline{N}.\underline{U}\right] dy \ , \tag{20}$$

with

$$\tilde{\sigma}(\underline{U}) = C : \nabla_y \underline{U}(y_1, y_2) \ , \tag{21}$$

∇_y being the (symmetric) gradient operator with respect to the space variables y_i.
In two dimensional elasticity, the incremental energy release rate is

$$G = \frac{\delta W}{\ell} \ . \tag{22}$$

The usual differential definition is the limit of the above ratio as $\ell \to 0$, it is known to vanish as $\lambda > 1/2$. In the present case it writes

$$G = k^2 a^{2\lambda-1} \frac{K(\mu) - K(0)}{\mu} + \ldots = k^2 \ell^{2\lambda-1} \frac{K(\mu) - K(0)}{\mu^{2\lambda}} + \ldots \tag{23}$$

The right hand side expression involves $\ell^{2\lambda-1}$ and recalls that obtained in the classical case (see (31) below). The function $K(\mu)$ depends on the notch opening angle ω, it is omitted in the above equations for simplicity.

2.4. Computation of $K(\mu)$

The function $\underline{V}^1(y_1, y_2, \mu)$ (either with $\mu = 0$ or $\mu > 0$) is the solution to an ill-posed problem (within the classical framework of the Lax-Milgram theorem) due to an unbounded energy. It is defined on an unbounded domain and must behave like $\rho^\lambda \underline{u}(\varphi)$ at infinity. The splittings (12) and (19) are necessary to ensure the existence of the solutions. Nevertheless, from a numerical point of view, the domain Ω^{in} must be artificially bounded at a large distance Δ (compared to 1, the dimensionless notch tip radius and to μ, the dimensionless crack length, say $\Delta = 100 \times \mathrm{Max}(1, \mu)$ for example, Figure 3). Then the finite element approximation $\underline{V}^{1h}(y_1, y_2, \mu)$ to $\underline{V}^1(y_1, y_2, \mu)$ can be computed directly, the behaviour at infinity being prescribed on the fictitious boundary Γ^Δ either as a Dirichlet condition

$$\underline{V}^{1h}(y_1, y_2, \mu) = \rho^\lambda \underline{u}(\varphi) \text{ on } \Gamma^\Delta \ , \tag{24}$$

or as a Neumann one

$$\tilde{\sigma}(\underline{V}^{1h}).\underline{n}^\Delta = \tilde{\sigma}(\rho^\lambda \underline{u}(\varphi)).\underline{n}^\Delta \text{ on } \Gamma^\Delta \ , \tag{25}$$

where $\underline{n}^\Delta$ is the outer normal to Γ^Δ. Then $K(\mu)$ is computed using the contour integral ψ (see (18), (20)). For simplicity, the selected contour is the fictitious outer boundary Γ^Δ. Even if the computation of $K(\mu)$ is not accurate, the computation of the difference $K(\mu) - K(0)$ is, by balancing the errors. An algorithmic approach for the computation of $K(\mu)$ is given in Appendix A.

The next section is not strictly in the scope of the paper. Nevertheless, it introduces useful notations for a following calculation (Section 3.1). In addition it gives an interesting result concerning an expression of the stress intensity factor at the tip of a short crack emanating from a sharp or a rounded v-notch. The reasoning is the same, the roles of the small parameters a and ℓ are simply exchanged.

2.5. Stress intensity factor at the tip of the new crack

An analogous result could have been obtained by expanding first with respect to the crack extension length. However, this will lead to a dimensionless crack length equal to 1 in the stretched domain Ω^{in} and a variable notch tip radius $1/\mu$. Indeed, it is numerically easier (automatic meshing) to have a constant notch radius and a variable crack length.

Nevertheless, this remark offers a method to determine the classical mode I stress intensity factor (SIF) k_I at the tip of a new short crack of given length ℓ. Let us consider the near field expansion (13) with respect to the small parameter ℓ instead of a (the domain is stretched by $1/\ell$ instead of $1/a$)

Table 1. Computed values of the geometry term $\kappa_I(0)$ compared to known theoretical ones ($\omega = 0°$ and $180°$), for sharp notches of different openings ω.

ω (°)	0	30	60	90	120	150	180
$\kappa_I(0)$ (comp.)	1.01	1.01	1.02	0.99	0.95	0.90	0.81
$\kappa_I(0)$ (theor.)	1.						0.79

$$\underline{U}^a(x_1, x_2, \ell) = \underline{U}^0(0, 0, 0) + k\ \ell^\lambda[\bar{\rho}^\lambda \underline{u}(\varphi) + \underline{\hat{W}}^1(\bar{y}_1, \bar{y}_2, \bar{\mu})] + \dots\ , \tag{26}$$

with $\bar{y}_i = x_i/\ell$, $\bar{\rho} = r/\ell$ and $\bar{\mu} = 1/\mu = a/\ell$. The term $\underline{\hat{W}}^1(\bar{y}_1, \bar{y}_2, \bar{\mu})$ plays the role of $\underline{\hat{V}}^1(y_1, y_2, \mu)$ in (13). It is independent of the crack length (stretched to 1) but depends now on the stretched notch tip radius $\bar{\mu}$. It undergoes the classical mode I singularity at the tip of the new crack and expands as

$$\underline{\hat{W}}^1(\bar{y}_1, \bar{y}_2, \bar{\mu}) = \underline{\hat{W}}^1(0', 0', \bar{\mu}) + \kappa_I(\bar{\mu})\sqrt{\rho'}\ \underline{u}^I(\varphi') + \dots \tag{27}$$

The singularity is expressed in terms of the local stretched polar coordinates $\rho' = r'/a$ and φ' (the prime denotes coordinates with origin at the tip O' of the new crack).

The coefficient $\kappa_I(\bar{\mu})$ is a geometry parameter. It is independent of the global geometry of the structure as well as of the applied loads (see the remark at the end of Section 2.2) but depends on the opening ω and on the dimensionless stretched notch tip radius $\bar{\mu}$. As a particular case, $\kappa_I(0)$ corresponds to a crack emanating from a sharp notch (see Table 1).

In physical (i.e., unstretched) coordinates, the expansion at the tip of the new crack is

$$\underline{U}^a(x_1', x_2', \ell) = \underline{U}^a(0', 0', \ell) + k_I\sqrt{r'}\ \underline{u}^I(\varphi') + \dots \tag{28}$$

Then using (26)–(28) leads to

$$k_I = k\ \ell^{\lambda-1/2}\kappa_I(\bar{\mu}) + \dots \tag{29}$$

This relation highlights the dependency in the crack length ℓ of the actual stress intensity factor k_I and the influence of the notch singularity through its generalized intensity factor k and the exponent λ.

Table 1 gives values of the geometry term $\kappa_I(0)$ corresponding to a crack emanating from a sharp notch ($\bar{\mu} = 0$). They are computed using a contour integral ψ like (20) (Leguillon and sanchez-Palencia, 1987) and compared to known theoretical data.

For $\omega = 0°$, i.e., a straight growing crack, $\kappa_I(0) = 1$ corresponds to the leading term of an expansion of k_I in powers of the extension length (Amestoy and Leblond, 1992). Equation (29) reduces to $k_I = k + \dots$

For $\omega = 180°$, the theoretical value $\kappa_I(0) = 0.79$ derives from the well known formula giving the stress intensity factor at the tip of a crack at a stress free edge in a half-space (Lawn, 1993) (keep in mind the normalization (8) and see the remark in Section 3.2).

3. The crack onset criterion at a sharp notch

3.1. A BRIEF REVIEW OF THE CRITERION

At a perfectly sharp notch $a = 0$, the criterion (Leguillon, 2002) is also a consequence of an expansion of the solution with respect to the crack extension length ℓ (Section 2.5). In that case it is the single small parameter. As above, the change of variables $\bar{y}_i = x_i/\ell$ leads to the near field expansion (see (26))

$$\begin{aligned} \underline{U}^0(x_1, x_2, \ell) &= \underline{U}^0(\ell\bar{y}_1, \ell\bar{y}_2, \ell) \\ &= \underline{U}^0(0, 0, 0) + k\ell^\lambda[\bar{\rho}^\lambda \underline{u}(\varphi) + \underline{\hat{W}}^1(\bar{y}_1, \bar{y}_2, 0)] + \dots \end{aligned} \tag{30}$$

The incremental energy release rate writes (see (23))

$$G = k^2\ell^{2\lambda-1}\bar{K} + \dots \ , \tag{31}$$

the scaling coefficient $\bar{K}$ being defined by

$$\begin{aligned} \bar{K} &= \psi(\underline{\hat{W}}^1(\bar{y}_1, \bar{y}_2, 0), \bar{\rho}^\lambda \underline{u}(\varphi)) \\ &= \psi(\underline{W}^1(\bar{y}_1, \bar{y}_2, 0), \bar{\rho}^\lambda \underline{u}(\varphi)) \ , \end{aligned} \tag{32}$$

since as in (12)

$$\underline{W}^1(\bar{y}_1, \bar{y}_2, 0) = \bar{\rho}^\lambda \underline{u}(\varphi) + \underline{\hat{W}}^1(\bar{y}_1, \bar{y}_2, 0) \ . \tag{33}$$

As before, $\bar{K}$ is also a function of the notch opening angle ω, it is omitted for simplicity.

The incremental Griffith criterion writes

$$G \geq G_c \ , \tag{34}$$

where G_c is the toughness of the material. It derives directly from the energy balance. It is almost unquestionable and an immediate consequence is that the crack jumps from 0 to ℓ (Leguillon, 2002). The condition (34) together with (31) gives a lower bound of this admissible crack jump length

$$\ell^{2\lambda-1} \geq \frac{G_c}{k^2\bar{K}} \qquad (2\lambda - 1 > 0) \ . \tag{35}$$

On the other hand the tension σ_n acting along the bisector at a distance ℓ of the tip (i.e., at the point with coordinates $x_1 = 0$, $x_2 = \ell$), prior to crack onset, writes at the leading order (see (8))

$$\sigma_n(0, \ell, 0) = k\ell^{\lambda-1} \ . \tag{36}$$

Associated with the strength criterion, we wish to find an ℓ so that it is not very large and satisfies:

$$\sigma_n \geq \sigma_c \ , \tag{37}$$

where σ_c denotes the strength of the material, this equation provides an upper bound for the crack jump length

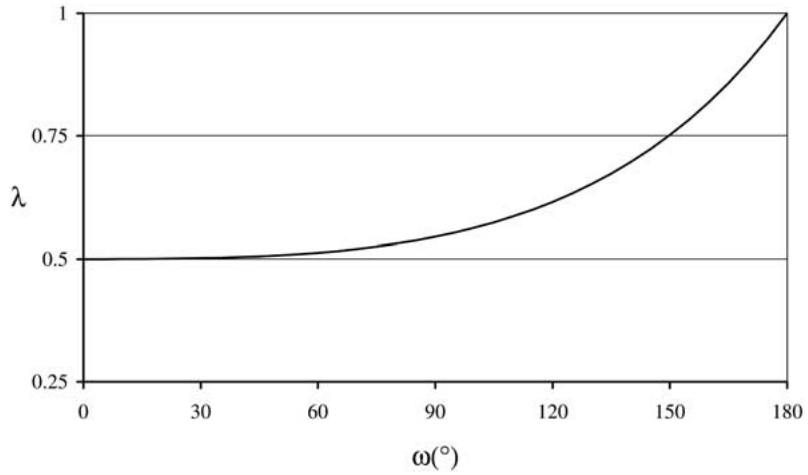

Figure 4. The singular exponent λ.

$$\ell^{1-\lambda} \leq \frac{k}{\sigma_c} \qquad (1-\lambda > 0)\ . \tag{38}$$

The consistency between the two conditions (35) and (38) leads to an admissible length

$$\ell_0 = \frac{G_c}{\bar{K}\sigma_c^2}\ , \tag{39}$$

and the resulting criterion for crack onset at a sharp notch is

$$k \geq k_c = \left(\frac{G_c}{\bar{K}}\right)^{1-\lambda} \sigma_c^{2\lambda-1}\ . \tag{40}$$

It is an Irwin-like criterion involving the generalized intensity factor k and its critical value k_c expressed in terms of two materials parameters: the toughness G_c and the strength σ_c. The use of (40) requires the knowledge of $\bar{K}$ which can be computed for each ω at $a = 0$.
Remark: Different angles lead to different units for the generalized intensity factors, it is not a severe drawback of the method. The aim of this work is to predict failure and the generalized intensity factor must be compared to a known critical value with the same units. The computation of this factor is now available or can be easily implemented in finite element codes. This approach is used by Dunn and other authors (Dunn et al., 1997; Reedy and Guess, 1993, 1997, 1999; Qian and Akisanya, 1998).

3.2. Computation of $\bar{K}$

The procedure described in Section 2.4 is used to compute directly $\underline{W}^1(\bar{y}_1, \bar{y}_2, 0)$ (instead of $\underline{\hat{W}}^1(\bar{y}_1, \bar{y}_2, 0)$) and then $\bar{K}$ using the contour integral (18). Nevertheless, if there is no crack at all, then theoretically $\underline{\hat{W}}^1(\bar{y}_1, \bar{y}_2, 0) = 0$ and $\bar{K} = 0$. Unfortunately, it is not numerically true since $\bar{K}$ is extracted from $\underline{W}^1(\bar{y}_1, \bar{y}_2, 0)$ (not from $\underline{\hat{W}}^1(\bar{y}_1, \bar{y}_2, 0)$). It remains an error $\bar{K}_e$. Then an accurate value of $\bar{K}$ is obtained by balancing the errors

$$\bar{K} = \psi(\underline{W}^1(\bar{y}_1, \bar{y}_2, 0), \bar{\rho}^\lambda \underline{u}(\varphi)) - \bar{K}_e\ . \tag{41}$$

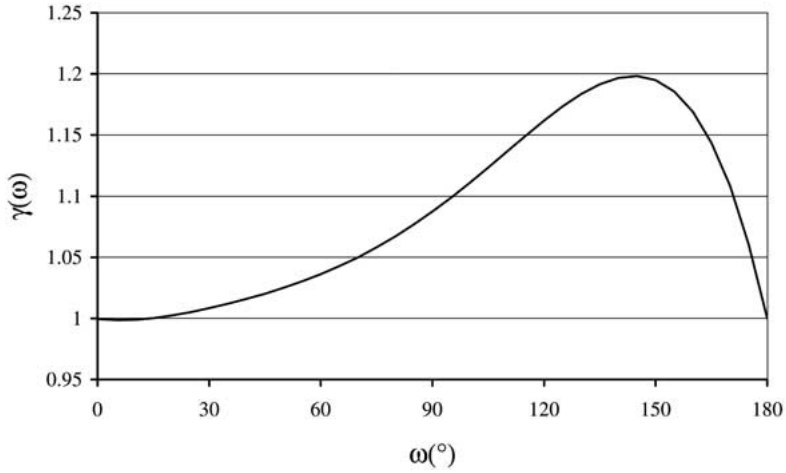

Figure 5. The universal function $\gamma(\omega)$.

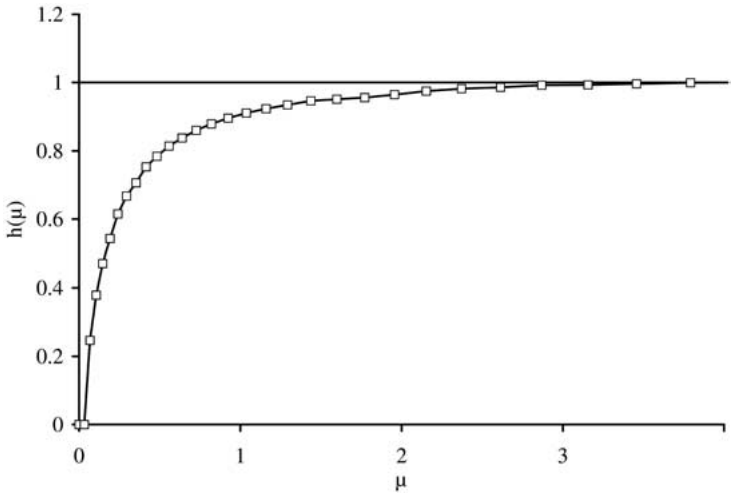

Figure 6. The function $h(\mu)$ (squares) for $\omega = 120°$ and its limit value 1. It is independent of the material stiffness.

Generally, the Dirichlet condition (24) tends to overestimate the value of $\bar{K}$ while the Neumann one (25) tends to underestimate it.
Remark: The normalization (8) is unusual for the classical opening crack mode I. For $\omega = 0$, $\varphi_0 = \pi$, $\lambda = 1/2$, it is traditionally

$$\sigma_n(\sqrt{r}\underline{u}^I(\pi)) = \frac{1}{\sqrt{2\pi r}} \ . \tag{42}$$

As a consequence, for $\omega = 0$, in plane strain elasticity and accounting for (8) and (42), the relation (31) is known to be

$$G = k_I^2 \times 2\pi \ \frac{1-\nu^2}{E} \ , \tag{43}$$

with an extra term 2π due to the normalization. Here E and ν denote respectively Young's modulus and Poisson's ratio of the material and $k = k_I$.
Then

$$\bar{K}_{|\omega=0} = 2\pi \, \frac{1-\nu^2}{E} \, . \tag{44}$$

Moreover, it is clear that $\bar{K}$ is proportional to $1/E$ whatever the opening ω. In addition, it has been checked that, for ν ranging from 0.1 to 0.4, deviations due to Poisson's ratio are almost negligible. Thus the criterion rewrites in a general form involving a universal function $\gamma(\omega)$

$$k \geq k_c = \gamma(\omega) E^{*\,1-\lambda} G_c^{1-\lambda} \sigma_c^{2\lambda-1} \, , \tag{45}$$

where we set

$$E^* = \frac{E}{2\pi(1-\nu^2)} \tag{46}$$

and then

$$\bar{K} = \frac{1}{E^* \gamma(\omega)^{1/(1-\lambda)}} \, . \tag{47}$$

Introducing the Irwin toughness parameter k_{Ic} equivalent to G_c through (43), the criterion (45) takes the simplified form

$$k \geq k_c = \gamma(\omega) k_{Ic}^{2(1-\lambda)} \sigma_c^{2\lambda-1} \, . \tag{48}$$

Figure 4 plots λ vs. the opening angle ω. In homogeneous materials this exponent is known to depend only on ω through the equation

$$\sin(\lambda(2\pi - \omega)) = \lambda \sin(\omega) \tag{49}$$

Figure 5 plots the universal function $\gamma(\omega)$. Thus together with Figure 4 and the material data, it defines the right hand side member of (45) (or (48)) (detailed numerical data are given in Appendix B).
Remark: Obviously, within the linear fracture mechanics framework, data are often scattered and inaccurate and a good and simple approximation is $\gamma(\omega) \simeq 1$ and

$$k \geq k_c = E^{*\,1-\lambda} G_c^{1-\lambda} \sigma_c^{2\lambda-1} = k_{Ic}^{2(1-\lambda)} \sigma_c^{2\lambda-1} \, . \tag{50}$$

Seweryn derived a similar formula (up to a multiplicative coefficient $\lambda \times 2^{2(1-\lambda)}$) based on Novozhilov's average stress argument (Seweryn, 1994; Novozhilov, 1969; Leguillon, 2002).

4. The crack onset criterion at a rounded notch

The criterion is still stated to be of the Irwin form (1). We propose herein to estimate the critical value of the generalized intensity factor k involved in the far field (7). It is a natural approach in computation of structures by finite elements for instance. The fine microstructure of the specimen is replaced by a simplified one ignoring the geometrical details and allowing reasonably reduced mesh sizes.

4.1. The criterion

As in the sharp notch situation, the idea is to get an admissible length ℓ_0 (see (39)) compatible with both the energy and the strength criteria. The incremental Griffith (energy) criterion reads (see (23))

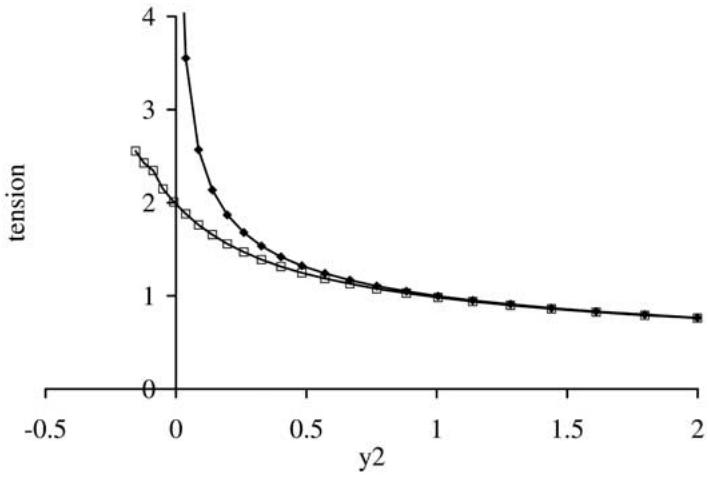

Figure 7. Comparison between the singular tension $y_2^{\lambda-1}$ (full diamonds) and $\tilde{\sigma}_n(\underline{V}^1(0, y_2, 0))$ (squares) along the bisector for $\omega = 120°$. It is independent of the material stiffness. The negative values of y_2 correspond to points located beyond the origin (see Figure 1(b)) in the spew filet.

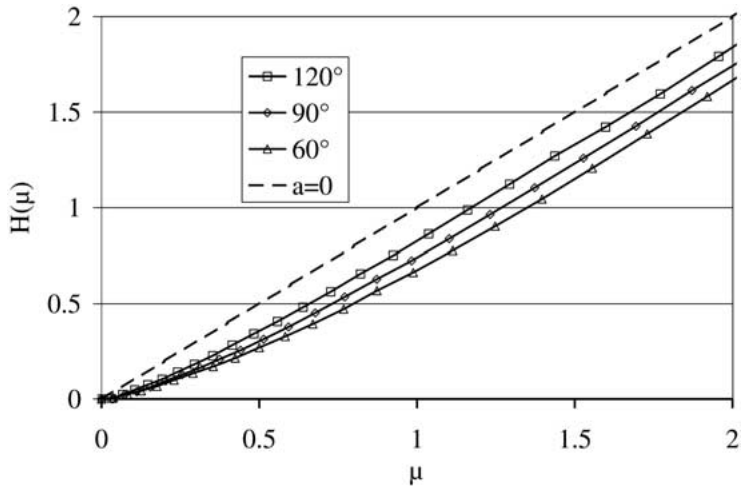

Figure 8. The function $H(\mu)$ for 3 different openings $\omega = 60°$ (triangles), $\omega = 90°$ (diamonds), $\omega = 120°$ (squares). The dotted line corresponds to the limit case of a perfectly sharp notch $a = 0$.

$$k^2 \ell^{2\lambda-1} \frac{K(\mu) - K(0)}{\mu^{2\lambda}} \geq G_c \ . \tag{51}$$

Regarding the remarks of Section 3.2 about the dependence of the scaling coefficient $\bar{K}$ on the elastic characteristics of the material which apply also to $K(\mu)$, we define $h(\mu)$ as follows:

$$h(\mu) = \frac{K(\mu) - K(0)}{\bar{K}\ \mu^{2\lambda}} \ , \tag{52}$$

where $\bar{K}$, defined by (47), corresponds to the perfectly sharp notch. The function $h(\mu)$ is independent of the elastic properties of the material. Since μ depends on ℓ, (51) is not an explicit equation giving a lower bound for the crack extension length ℓ. However, numerical computations show that $h(\mu)$ is an increasing function of μ, tending toward 1 as $\mu \to \infty$ as

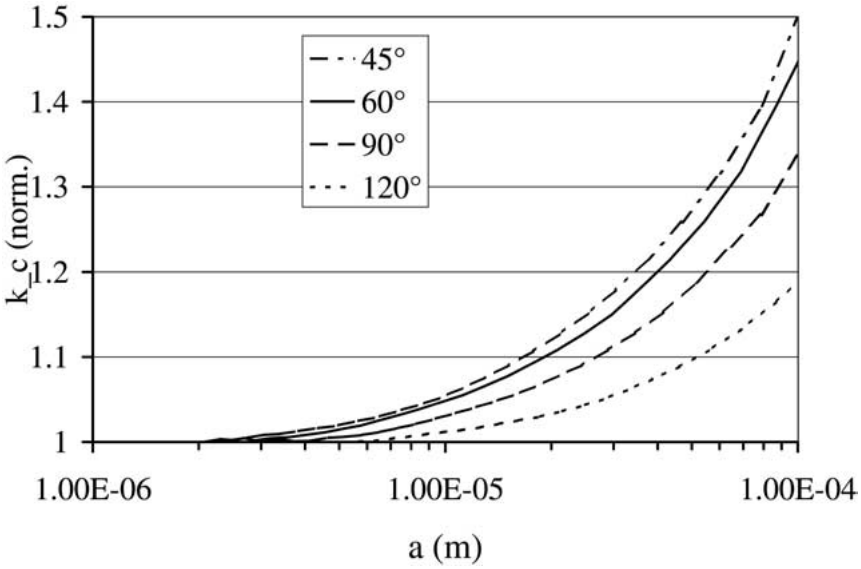

Figure 9. The normalized critical value k_c of the generalized intensity factor k for PMMA, as a function of the notch tip radius a, for 4 different notch openings: $\omega = 45°, 60°, 90°$ and $120°$.

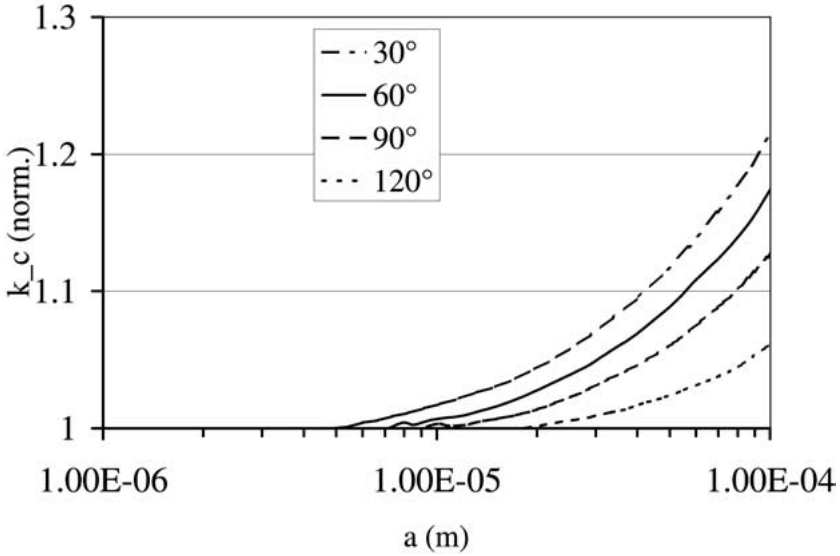

Figure 10. The normalized critical value k_c of the generalized intensity factor k for AZ, as a function of the notch tip radius a, for 4 different notch openings: $\omega = 30°, 60°, 90°$ and $120°$.

expected (see Figure 6 plotted for the opening $\omega = 120°$). Thus, (51) can be used to compute a lower bound for ℓ, for any given notch tip radius a.

On the other hand, from (10)–(12), the tension along the bisector at a distance ℓ of the origin, prior to any crack nucleation can be expressed as

$$\sigma_n(\underline{U}^a(0, \ell, 0)) = ka^{\lambda-1}\tilde{\sigma}_n(\underline{V}^1(0, \mu, 0)) + \dots \tag{53}$$

Once again, the stress criterion

$$\sigma_n(\underline{U}^a(0, \ell, 0)) \geq \sigma_c \ , \tag{54}$$

together with (53) does not bring an explicit upper bound for ℓ. It is numerically checked that $\tilde{\sigma}_n(\underline{V}^1(0,\mu,0))$ is a decreasing function of μ and then (53) can be used to compute this upper bound for a fixed a. Figure 7 exhibits $\tilde{\sigma}_n(\underline{V}^1(0,y_2,0))$ compared to $y_2^{\lambda-1}$ (keep in mind the normalization (8)) along the bisector, for $\omega = 120°$. It is independent of the material stiffness. Clearly, the singularity disppears in case of a rounded notch, the actual stress field remains bounded (Figure 7). Nevertheless, the solution recovers very quickly the elastic far field (for $y_2 \geq 1$ in the case of Figure 7) explaining the influence of the singular far field on the non singular local solution.
Remark: Indeed, for a fixed a, if ℓ and then μ increase, the influence of the notch tip radius becomes negligible and the limit recovers the sharp notch case as shown on Figures 6 and 7. Very neighbouring figures are obtained for the other openings $\omega = 60°$ and $90°$.

The consistency between these two bounds leads to an admissible crack extension length ℓ_0 and to a relation between a and ℓ_0

$$a\ \bar{K}\, H(\mu_0) = \frac{G_c}{\sigma_c^2}\ , \tag{55}$$

where $\mu_0 = \ell_0/a$ and

$$H(\mu) = \frac{\mu^{2\lambda-1} h(\mu)}{\tilde{\sigma}_n(\underline{V}^1(0,\mu,0))^2}\ . \tag{56}$$

The function $H(\mu)$ is independent of the elastic properties of the material, it is plotted in Figure 8.
Remark: As $\mu \to \infty$ or what is equivalent as $a \to 0$ then $h(\mu) \to 1$ (Figure 6) and $\tilde{\sigma}_n(\underline{V}^1(0,\mu,0)) \to \mu^{\lambda-1}$ (Figure 7). As a consequence $H(\mu) \to \mu$ and (55) recovers the relation (39) providing ℓ_0 in case of a perfectly sharp notch.

The notch tip radius a being prescribed, (55) gives ℓ_0. Inserted in (51) or in (54), it leads finally to a critical value k_c of the generalized intensity factor k (as a function of a). It is plotted for the two different materials in Figures 9 and 10 in a normalized form defined by

$$k_c(\text{norm.}) = k_c / k_{c\,|a=0}\ , \tag{57}$$

the value 1 refers to the limit corresponding to the perfectly sharp notch $a = 0$. It is hazardous to consider radii larger than 100 μm since they must be small (asymptotic assumption) compared to the notch depth. The influence of the notch tip radius decreases as the notch opening ω increases. This influence vanishes (and the corresponding curve in Figures 9 and 10 would be flat) for a straight edge ($\omega = 180°$), indeed the notch tip radius is meaningless in that case.
Remark: The procedure proposed above cannot be extended to very small openings and eventually to a primary crack ($\omega = 0°$), this is obvious from the stretched domain Ω^{in} (Figure 3). The distance between the origin O (the sharp notch tip) and the rounded boundary increases and tends to infinity as ω decreases, since the stretched radius is 1 whatever its actual value. Another approach must be used, the notch faces must be shifted giving rise to boundary layers.

4.2. Comparison with the experimental results of Dunn et al. on PMMA specimens

Dunn et al. (1997) performed 3-point flexure experiments on a notched specimen of PMMA ($E = 2.3$ GPa, $\nu = 0.36$, $\sigma_c = 124$ MPa, $G_c = 394$ J.m^{-2}). By varying the specimen height, the notch depth and the notch opening they showed that the Irwin-like criterion (1) is

Table 2. Comparison of the critical intensity factor values k_c for PMMA, 1) experiments 2) perfectly sharp notch prediction (45) (or (48)), 3) corrected prediction accounting for the notch tip radius. Unit for k_c is MPa.m$^{1-\lambda}$ and thus differs from one line to another.

ω	k_c exp.	From	k_c (45)	a (μm)	corrected k_c
30°			0.42	25.4	0.48
45°	0.59	(Yosibash et al., 2003)	0.44	30	0.55
60°	0.57	(Dunn et al., 1997)	0.49	25.4	0.56
90°	0.89	(Dunn et al., 1997)	0.74	25.4	0.82
120°	1.91	(Dunn et al., 1997)	1.77	25.4	1.85

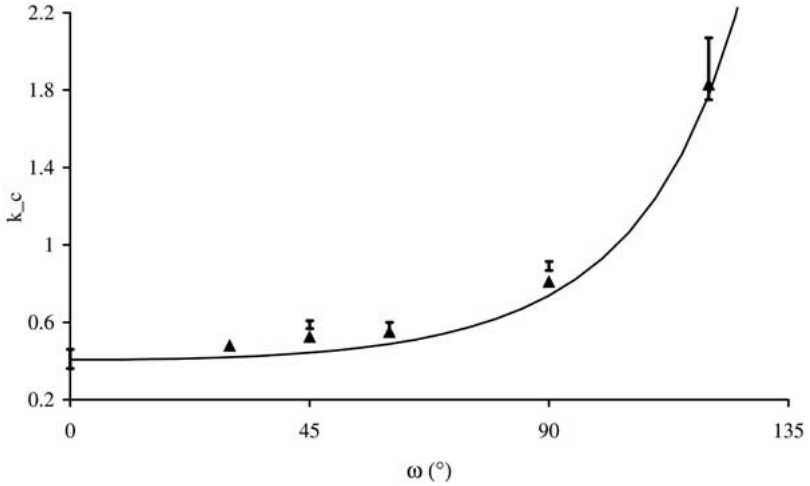

Figure 11. Comparison with experiments by Dunn et al. on PMMA specimens (all results are from Dunn et al. except $\omega = 45°$ from Yosibash et al.), 1) experiments (error bars), 2) prediction using the sharp notch criterion (solid line), 3) correction for a notch tip radius $a = 25.4$ μm ($a = 30$ μm for $\omega = 45°$) (full triangles).

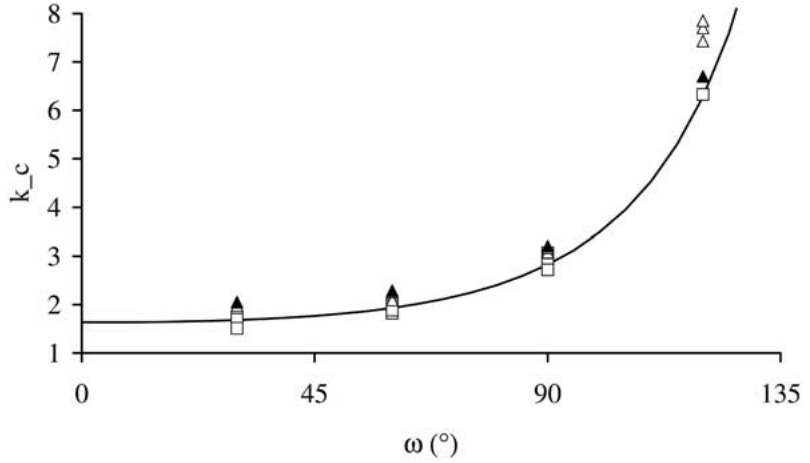

Figure 12. Comparison with experiments by Yosibash et al. on AZ specimens, 1) $a = 60$ μm (squares), 2) $a = 100$ μm (triangles), 3) prediction using the sharp notch criterion (solid line), 4) correction for a notch tip radius $a = 100$ μm (full triangles).

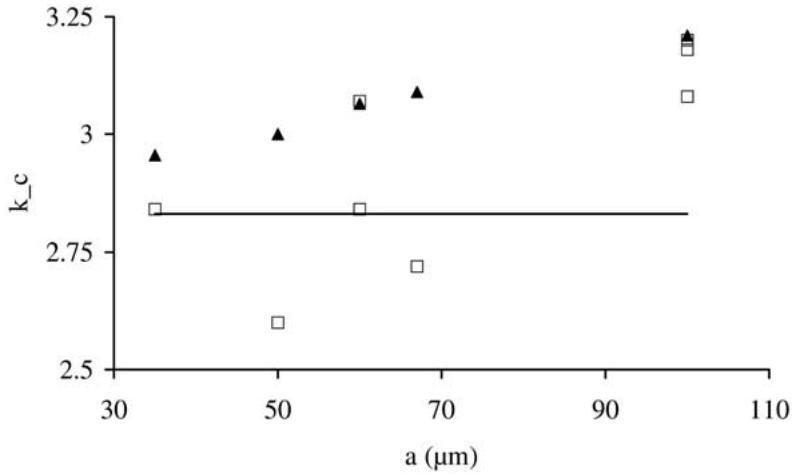

Figure 13. Detailed comparison between experiments and theoretical predictions on AZ specimens for $\omega = 90°$. 1) Experiments (squares), 2) perfectly sharp notch prediction (solid line), 3) correction accounting for the notch tip radius (full triangles).

the appropriate one to predict failure. They determined experimentally the critical values of k_c. In a first step these values are estimated using the sharp notch criterion (45) (or (48)), it is clear that the prediction underestimates slightly the experimental values. In a second step, the correction suggested in Figure 9 is applied for a notch tip radius $a = 25.4$ μm as reported in the paper of Dunn. The predicted values using the sharp notch criterion must be increased by 13.5%, 11% and 4.7%, respectively, for $\omega = 60°$, $90°$ and $120°$. Table 2 summarizes these results, and Figure 11 presents the comparison between the experimental results and the predicted values by the failure criterion before and after the v-notch radius tip correction. The correction still underestimates the measures. The remaining (small) discrepancy is certainly due to plasticity and crazing effects.

4.3. Comparison with the experimental results of Yosibash et al. on Alumina-Zirconia specimens

Yosibash et al. (2002) worked out similar experiments on notched specimen of a ceramic material made of Alumina/Zirconia (Al_2O_3/7% ZrO_2). Many specimens have been tested with slight changes on Young's modulus and different notch tip radii. Among them, for simplicity we selected those corresponding to the following parameters: $E = 350$ GPa, $\nu = 0.233$, $\sigma_c = 290$ MPa, $G_c = 45.4$ J.m^{-2}. The material is by far stiffer than the previous one studied in Section 4.2. The sharp notch prediction matches accurately with the experiments for a small notch tip radius ($a = 60$ μm) as observed on Figure 12. Figure 13 provides details of the measures and of the prediction for $\omega = 90°$. Despite the scattering, the efficiency of the initial sharp notch criterion and the correction is obvious.

On the other hand a misfit is visible for $\omega = 120°$ for a large notch tip radius $a = 100$ μm between the corrected value and the measures. In the model, the measures would correspond to a larger notch tip radius $a \simeq 340$ μm. The question is now: how accurate is the determination of this radius?

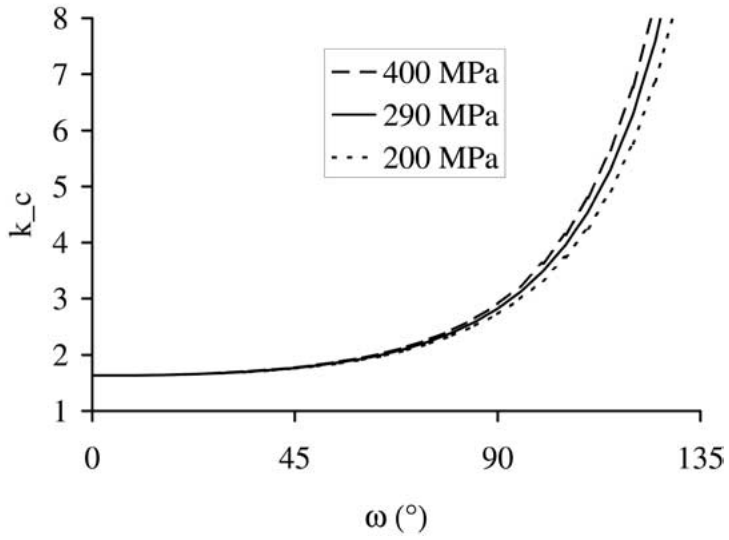

Figure 14. Comparison at small openings of sharp notch predictions in AZ for different values of the strength: $\sigma_c = 290$ MPa (solid line), $\sigma_c = 200$ MPa (bottom dotted line), $\sigma_c = 400$ MPa (top dotted line).

5. Conclusion

All this reasoning is based on the smallness of the notch tip radius and the crack extension length allowing asymptotics of the solution. They must be small with respect to the notch depth and as a consequence small compared to any characteristic length of the specimen. In the experiments on PMMA specimens, $a \simeq 30$ μm and, using (39), ℓ_0 is found to be around 20 μm, thus they are from 60 to 200 times smaller than the notch depth depending on the specimen geometry (the notch depth ranges from 1.78 to 7.11 mm). This is also true for AZ specimen tests, the notch depth is 5 mm and then 50 times larger than the largest examined tip radius $a = 100$ μm leading to $\ell_0 \simeq 60$ μm (ℓ_0 ranges from 40 to 60 μm depending on the opening ω and the radius a). As a consequence, the corrections are necessary small and the initial prediction based on the assumption of a sharp notch is still a satisfying approximation of the critical intensity factor values.

The criterion requires the knowledge of two fracture parameters, the toughness G_c and the strength σ_c. Volume effects and surface roughness make this second parameter difficult to determine. Nevertheless, for openings lower than 135°, the robustness of the criterion is shown in Figure 14 where AZ sharp notch predictions are plotted for 3 different values of σ_c. The influence of the measured σ_c arises to be small at small and medium openings. Of course, the difference would be more significant for large openings leading to a flat geometry close to the unnotched case.

Regarding Figure 11, it is clear that, in PMMA specimens, the criterion underestimates (as expected) slightly the experimental results and the correction accounting for a notch tip radius brings an improvement in the prediction. Below $a = 5$ μm Figure 9 shows that no correction is necessary. For $a = 25.4$ μm the correction ranges between 5% and 13%. The remaining discrepancy is probably due to micro-mechanisms effects neglected in this analysis (plasticity and crazing). It must be pointed out that the inital crack length ℓ_0 is of same order of magnitude than the estimated process zone size but not smaller. The tensile stress is calculated at this distance, i.e., in the elastic field just outside the process zone.

Table 3. The elastic singularity exponent λ and the universal function γ as functions of the notch opening ω.

ω (°)	λ	$\gamma(\omega)$	ω (°)	λ	$\gamma(\omega)$
0	0.500	1.00	90	0.545	1.09
5	0.500	1.00	95	0.553	1.10
10	0.500	1.00	100	0.563	1.11
15	0.500	1.00	105	0.574	1.12
20	0.501	1.00	110	0.586	1.14
25	0.501	1.01	115	0.600	1.15
30	0.502	1.01	120	0.615	1.16
35	0.503	1.01	125	0.633	1.17
40	0.504	1.02	130	0.652	1.18
45	0.506	1.02	135	0.673	1.19
50	0.507	1.03	140	0.697	1.20
55	0.510	1.03	145	0.723	1.20
60	0.513	1.04	150	0.752	1.19
65	0.516	1.04	155	0.784	1.19
70	0.520	1.05	160	0.819	1.17
75	0.525	1.06	165	0.858	1.14
80	0.531	1.07	170	0.901	1.11
85	0.537	1.08	175	0.948	1.06
			180	1.000	1.00

A conclusion for AZ specimens is not so straightforward. A comparison between Figures 9 and 10 reveals that for a given notch tip radius, stiffer is the material and smaller is the the correction. For an opening $\omega = 60°$ and a notch tip radius of 100 μm, the correction does not exceed 18% for AZ while it is 45% for PMMA. The limit below which no correction is necessary is $a = 10$ μm in AZ specimens, it is twice smaller than in PMMA. This could give way to the temptation to draw the conclusion that stiffer is the material and more insensitive it is to small notch radii. Unfortunately, measures for $\omega = 120°$ and $a = 100$ μm tend to weaken this statement. They are 22% above the sharp notch prediction and still 14% above the corrected one.

Appendix A. The algorithm for computing $\underline{V}^1(y_1, y_2, \mu)$ and $K(\omega, \mu)$.

A key component in the proposed failure criteria is the computation of $K(\omega, \mu)$, according to (18). Herein a detailed algorithm for its computation by means of numerical methods is presented, for a given opening angle ω_0.

– Take $a = 0$ (sharp v-Notch), and compute the eigen-pairs λ and $\underline{u}(\varphi)$ for the given ω_0 (see methods for computations in (Leguillon and Sanchez-Palencia, 1987) or (Yosibash and Szabo, 1995) for example). For isotropic materials λ and $\underline{u}(\varphi)$ can be obtained analytically.

- Using the finite element method, construct a domain as shown in Figure 3(b), with a v-Notch tip radius of 1 and a crack of length μ (this will vary). Take the outer radius of the domain to be $\Delta = 100 \times \text{Max}(1, \mu)$.
- On the outer circular boundary prescribe the boundary conditions $\Delta^{\lambda}\underline{u}(\varphi)$ as essential boundary conditions, or compute the corresponding traction and prescribe these instead.
- Solve the elastic system of equations and obtain the solution denoted by $\underline{V}^1(y_1, y_2, \mu)$.
- Now, substitute $\underline{V}^1(y_1, y_2, \mu)$ and $\rho^{\lambda}\underline{u}(\varphi)$ in (18), with the integration taken along a circular sector of given radius (or any other contour). For simplicity, select the circular outer boundary of the domain as the path of integration. The obtained value is $K(\omega_0, \mu)$.
- Repeat steps above for various values of μ (various crack length sizes) to generate $K(\omega_0, \mu)$).
- Report the values in (55) to get a relation between the notch tip radius a and μ and then ℓ.

Appendix B. The functions $\gamma(\omega)$ and λ.

Values are numerically determined using the procedure proposed in (Leguillon and Sanchez-Palencia, 1987) for λ and in Section 3 for γ. Curves are then smoothed and a small discrepancy on the last digit of λ can be sometimes observed when compared to data from other origins. Nevertheless, the accuracy provided in Table 3 is by far sufficient to determine the critical value of the criterion (45) (or (48)).

References

Amestoy, M. and Leblond, J.B. (1992). Crack paths in plane situations – II. Detailed form of the expansion of the stress intensity factors. *International Journal of Solids and Structures* **29**(4), 465–501.

Dunn, M.L., Suwito, W. and Cunningham, S. (1997). Fracture initiation at sharp notches: correlation using critical stress intensities. *International Journal of Solids and Structures* **34**(29), 3873–3883.

Hashin, Z. (1996). Finite thermoelastic fracture criterion with application to laminate cracking analysis. *Journal of Mechanics and Physics of Solids* **44**, 1129–1145.

Lawn, B. (1993). *Fracture of brittle solids – Second Edition*. Cambridge Solid State Science Series, Cambridge University Press, Cambridge.

Leguillon, D. (1989). Calcul du taux de restitution de l'énergie au voisinage d'une singularité. *C.R. Acad. Sci. Paris* **309**(II), 945–950.

Leguillon, D. (2002). Strength or toughness? A criterion for crack onset at a notch. *European Journal of Mechanics A/Solids* **21**, 61–72.

Leguillon, D. and Sanchez-Palencia, E. (2002). *Computation of Singular Solutions in Elliptic Problems and Elasticity*. J. Wiley, New-York and Masson, Paris.

Leguillon, D. and Siruguet, K. (2002). Finite fracture mechanics – Application to the onset of a crack at a bimaterial corner. *In* Proceedings of the IUTAM symp. on Analytical and computational fracture mechanics of non-homogeneous materials, Cardiff, 18–22 June 2001, Kluwer Academic Press, Dordrecht: 11–18.

Mohammed, I. and Liechti, K.M. (1969). Cohesive zone modeling of crack nucleation at bimaterial corners. *Journal of Mechanics and Physics of Solids* **48**, 735–764.

Novozhilov, V.V. (1969). On a necessary and sufficient criterion for brittle strength. *Journal of Applied Mathematics and Mechanics. (Translation of PMM)* **33**, 212–222.

Qian, Z. and Akisanya, A.R. (1998). An experimental investigation of failure initiation in bonded joints. *Acta Mater.* **46**, 4895–4904.

Reedy, E.D. and Guess, T.R. (1993). Comparison of butt tensile strength data with interface corner stress intensity factor prediction. *International Journal of Solids and Structures* **30**(21), 2929–2936.

Reedy, E.D. and Guess, T.R. (1997). Interface corner failure analysis of joint strength: effect of adherend sitffness. *International Journal of Fracture* **88**, 305–314.

Reedy, E.D. and Guess, T.R. (1999). Additional interface corner toughness data for an adhesively-bonded butt joint. *International Journal of Fracture* **98**, L3–L8.

Seweryn, A. (1994). Brittle fracture criterion for structure with sharp notches. *Engineering Fracture Mechanics* **47**(5), 673–681.

Yosibash, Z. and Szabo, B.A. (1995). Generalized stress intensity factors in linear elastostatics. *International Journal of Fracture* **72**, 223–240.

Yosibash, Z., Bussiba, A. and Gilad I. Failure criteria for brittle elastic materials. Submitted for publication in *International Journal of Fracture*.